Inorg. Chem. **2002**, *41*, 2583–2591

Synthesis and Characterization of Dimetallic Oxorhenium(V) and Dioxorhenium(VII) Compounds, and a Study of Stoichiometric and Catalytic Reactions

James H. Espenson,* Xiaopeng Shan, Ying Wang, Ruili Huang, David W. Lahti, JaNeille Dixon, Gábor Lente,† Arkady Ellern, and Ilia A. Guzei‡

Ames Laboratory and Department of Chemistry, Iowa State University of Science and Technology, Ames, Iowa 50011

Received December 18, 2001

Chelating dithiolate ligands—e.g., mtp from 2-(mercaptomethyl)thiophenol, edt from 1,2-ethanedithiol, and pdt from 1,3-propanedithiol—stabilize high-valent oxorhenium(V) against hydrolytic and oxidative decomposition. In addition to the dithiolate chelating to a single rhenium, one sulfur forms a coordinate bond to the other rhenium. In one arrangement this gives a dimer with a nearly planar diamond core with different internal Re–S distances. The new compounds are $\{MeReO(edt)\}_2$ (**2**) and $\{MeReO(pdt)\}_2$ (**3**), which can be compared to the previously known $\{MeReO(mtp)\}_2$ (**1**). Another mode of synthesis leads to $\{ReO\}_2(mtp)_3$ (**5**) and $\{ReO\}_2(edt)_3$ (**6**). They, too, have similar Re_2S_2 cores that involve donor atoms from two of the dithiolate ligands; the third dithiolate chelates one of the rhenium atoms. Gentle hydrolysis of **1** affords $[Bu^n4][\{MeReO(mtp)\}_2(\mu\text{-OH})]$ (**7**) in low yield. It appears to be the first example of this structural type for rhenium. The use of dithioerythritol as a starting material allowed the synthesis of a dioxorhenium(VII) compound, $\{MeReO_2\}_2(dte)$ (**8**). Its importance lies in understanding the role such compounds are believed to play as intermediates in oxygen atom catalysis. Ligation of the dimers **1**–**3** converts them into monomeric compounds, MeReO(dithiolate)L. These reactions go essentially to completion for L = PPh_3, but reach an equilibrium for L = NC_5H_4R. With R = 4-Ph, the values of $K/10^3$ L mol^{-1} for the reactions (**1**–**3**) + 2L = 2MeReO(dithiolate)L are identical within 3σ: 1.15(3) (**1**), 1.24(4) (**2**), and 1.03(16) (**3**). The rates of monomer formation follow the rate law $-\text{d ln [dimer]/dt} = k_a[L] + k_b[L]^2$. These trends were found: (1) phosphines are slow to react compared to pyridines, (2) the edt dimer **2** reacts much more rapidly than **1** and **3**. Dimer **1** and MeReO(mtp)PPh_3 both catalyze oxygen atom transfer: PicO + PPh_3 → Pic + Ph_3PO. Compound **1** is ca. 90 times more reactive, which can be attributed to its lability toward small ligands as opposed to the low rate of displacement of PPh_3 from the mononuclear catalyst. The kinetics of this reaction follows the rate law $-\text{d[PicO]/dt} = k[\text{PicO}][\mathbf{1}]/\{1 + \kappa[PPh_3]\}$, with $k = 5.8 \times 10^6$ L mol^{-1} s^{-1} and $\kappa = 3.5 \times 10^2$ L mol^{-1} at 23 °C in benzene. A mechanism has been proposed to account for these findings.

Introduction

One of the first oxorhenium(V) compounds of the type referred to in the title is represented by the known compound $\{MeReO(mtp)\}_2$ (**1**, Chart 1).[1] The dinuclear core of this compound is a diamond-shaped unit. Dimer formation can be rationalized in terms of the need to provide a sufficient electron density and coordination number. Indeed, the reaction of **1** with different nucleophiles (L) produces monometallic compounds, MeReO(mtp)L, in which the new ligand provides the requisite electron density and coordination number.[2,3]

As this subject has developed, other compounds have naturally emerged and others were then made as deliberate targets. In this work we describe their preparation and characterization. As it turns out, more than one structure was encountered, but in each case the rhenium atoms remain five-coordinate, in an approximate square pyramid.

* Corresponding author. E-mail: espenson@ameslab.gov.
† Current address: Department of Inorganic and Analytical Chemistry, University of Debrecen, Debrecen, Hungary.
‡ Current address: Department of Chemistry, University of Wisconsin, Madison, WI 53706.

(1) Jacob, J.; Guzei, I. A.; Espenson, J. H. *Inorg. Chem.* **1999**, *38*, 1040−1041.
(2) Jacob, J.; Lente, G.; Guzei, I. A.; Espenson, J. H. *Inorg. Chem.* **1999**, *38*, 3762−3763.
(3) Lente, G.; Guzei, I. A.; Espenson, J. H. *Inorg. Chem.* **2000**, *39*, 1311−1319.

10.1021/ic011287j CCC: $22.00
Published on Web 04/09/2002

Chart 1. Structural Formulas for Crystallographically Characterized Compounds

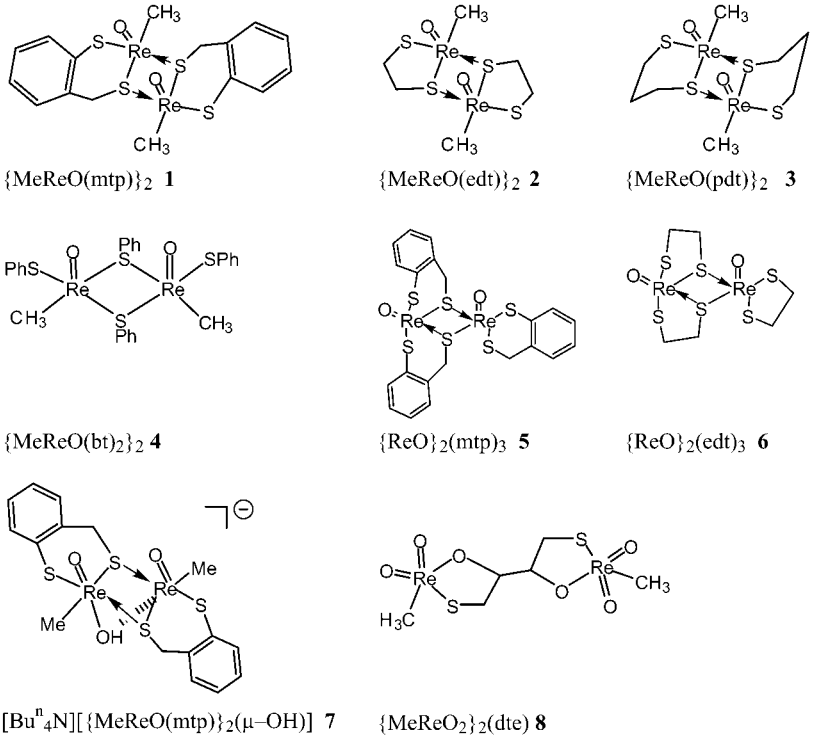

Included in this list of new compounds is one example of a dioxorhenium(VII) compound, which is significant because it models in a more stable form the transient intermediate in oxygen atom transfer (OAT) reaction catalyzed by **1**.[4] We have also studied the kinetics of selected reactions, stoichiometric and catalytic, some of which revealed significant differences. The most notable of these is the catalysis of reactions between pyridine *N*-oxides and phosphines, for which dinuclear oxorhenium(V) compounds such as {MeReO(mtp)}$_2$ provide substantially better pathways than the already facile ones provided by their mononuclear counterparts, MeReO(dithiolate)PPh$_3$. One objective of this research was to gain an understanding of the special accelerating effects of the dimers.

Experimental Section

The starting point for several of these syntheses was {MeReO(bt)$_2$}$_2$, **4**, where bt = benzenethiol.[5] Others were obtained from {MeReO(mtp)}$_2$, **1**.[1]

{MeReO(edt)}$_2$, 2. A solution containing **4** (87 mg, 0.1 mmol) and 2 mmol of Me$_2$S in 10 mL of toluene was supplied with 2.5 mmol of edtH$_2$ (ethane-1,2-dithiol), and then stirred for 4 h. The solution was concentrated to 1 mL by vacuum and 5 mL of hexane was layered on it. This produced a brown solid which was collected by filtration and washed with hexanes. The yield of **2** was 73%.

{MeReO(pdt)}$_2$, 3. The same procedure as above gave an 85% yield of **3**. A crystal suitable for X-ray analysis was grown from methylene chloride−hexanes.

{ReO}$_2$(mtp)$_3$, 5. 2-(Mercaptomethyl)thiophenol (3.0 g, 19 mmol) was added to a solution of dirhenium heptoxide (1.5 g, 3.1 mmol) in 20 mL of THF. The dark brown solution was left to stand at room temperature for 2.5 h. Then 70 mL of hexane was added, and the reaction mixture kept at −11 °C for 2 days. After filtering and extensive washing with hexane, the product was isolated in 85% yield as a dark solid. Yellow needle-shaped crystals suitable for X-ray diffraction analysis were obtained by slow evaporation of a benzene solution at room temperature for one week. This compound, under the designation **D$_1$**, has already been applied as a catalyst for the reaction between phosphines and molecular oxygen[6] (as such, it is one of few that activate O_2), and for the oxidation of phosphines, arsines, stibenes, sulfides, and dienes by pyridine *N*-oxides.[7]

{ReO}$_2$(edt)$_3$, 6. Benzenethiol (0.103 mL, 110 mg, 1.00 mmol) was added dropwise to a solution of rhenium(VII) oxide (48 mg, 0.1 mmol) in 20 mL of THF. This mixture was stirred for 6 h at room temperature. After 40 mL of hexanes was layered on the top, the mixture was kept in the freezer for 2 days. A dark solid, believed to be {MeReO}$_2$(bt)$_3$, was obtained. Its yield by this formula was 54%. It was then dissolved in 20 mL of toluene, after which ethane-1,2-dithiol (25 μL, 28 mg, 0.3 mmol) was added. This resulting solution was stirred for 2 h, concentrated to 2 mL under vacuum, layered by 10 mL of hexanes, and stored in the freezer for 2 days. This procedure gave a 39% yield, relative to the original Re_2O_7 taken, of the brown compound {ReO}$_2$(edt)$_3$, **6**. Crystals suitable for X-ray diffraction were obtained by recrystallization from methylene chloride−hexanes.

[Bu$^n_4$N][{MeReO(mtp)}$_2$(μ-OH)], 7. A benzene solution of yellow-brown **1** containing excess tetra-*n*-butylammonium chloride was layered over water. This reaction occurred:

$$\mathbf{1} + \mathrm{Bu}^n\mathrm{4NCl} + \mathrm{H_2O} \rightarrow [\mathrm{Bu}^n\mathrm{4N}][\{\mathrm{MeReO(mtp)}\}_2(\mu\text{-OH})] + \mathrm{HCl} \quad (1)$$

A solid formed and dichroic red-green crystals suitable for X-ray

(4) Wang, Y.; Espenson, J. H. *Inorg. Chem.* **2001**, *41*, ASAP.
(5) Takacs, J.; Cook, M. R.; Kiprof, P.; Kuchler, J. G.; Herrmann, W. A. *Organometallics* **1991**, *10*, 316−320.
(6) Huang, R.; Espenson, J. H. *J. Mol. Catal. A: Chem.* **2001**, *168*, 39−46.
(7) Huang, R.; Espenson, J. H. *Inorg. Chem.* **2001**, *40*, 994.

Table 1. Elemental Analyses (EA) and ^{1}H and ^{13}C NMR Data for Oxorhenium Dimers

compound	EA: exptl (calcd)	NMR (C_6D_6, 25 °C), δ
{MeReO(edt)}$_2$, **2**	C: 11.73 (11.82) H: 2.27 (2.39) S: 20.82 (20.93)	^{1}H: 3.65 (m, 2H), 2.62 (s, 6H), 2.37 (m, 2H), 2.24 (m, 2H), 1.92 (m, 2H) ^{13}C: 47.1, 36.6, 13.2
{MeReO(pdt)}$_2$, **3**	C: 15.17 (14.85) H: 2.65 (2.80) S: 19.89 (19.83)	^{1}H: 2.84 (s, 6H), 2.65 (m, 4H), 2.43 (m, 2H), 2.18 (m, 4H), 2.08 (m, 2H) ^{13}C: 34.0, 33.1, 29.5, 19.6
{MeReO(mtp)}$_2$, **1**[a,b]	C: 26.68 (25.85) H: 2.53 (2.44) S: 17.33 (17.27)	^{1}H: 7.52 (d, 2H, J = 8 Hz), 7.03 (m, 2H), 6.91 (m, 4H), 4.05 (d, 2H, J = 10.8 Hz), 3.53 (d, 2H, J = 10.8 Hz), 2.91 (s, 6H) ^{13}C: 141.94, 135.81, 130.62, 130.56, 130.18, 127.87, 36.91, 17.10
{ReO}$_2$(mtp)$_3$, **5**	C: 31.70 (31.81) H: 2.45 (2.34) S: 21.03 (21.23)	^{1}H: 7.50−7.35 (m, 8H), 7.30−7.15 (m, 4H), 5.67 (d, 1H, CH_2, J = 11.2), 5.21 (d, 1H, CH_2, J = 11.2), 5.06 (d, 1H, CH_2, J = 12.4), 4.30 (d, 1H, CH_2, J = 11.6), 3.75 (d, 1H, CH_2, J = 12.4), 3.62 (d, 1H, CH_2, J = 11.2) ^{13}C: 140.92, 140.36, 139.71, 139.02, 135.70, 135.47, 131.07, 130.94, 130.90, 130.58, 130.56, 130.38, 129.22, 128.97, 128.85, 128.70, 128.54, 128.42, 42.29, 40.92, 38.90
{ReO}$_2$(edt)$_3$, **6**	C: 10.88 (10.58) H: 1.95 (1.78) S: 28.03 (28.28)	^{1}H: 3.34 (m, 2H), 3.02 (m, 2H), 2.70 (m, 4H), 2.49 (m, 4H) ^{13}C: solubility is too low
[Bu$^n_4$N][{MeReO(mtp)}$_2$(μ-OH)], **7**	c	^{1}H: 4.86 (d, 2H, J = 11.6 Hz); 3.87 (d, 2H, CH_2, J = 11.6 Hz); 2.50 (s, 3H)
{$MeReO_2$}$_2$(dte), **8**	C: 11.88 (11.69) H: 1.97 (1.96) S: 10.39 (10.40)	^{1}H: 4.29 (m, 2H), 2.94 (m, 4H), 2.26 (s, 6H) ^{13}C: 34.0, 33.1, 29.5, 19.6

[a] From ref 1. [b] IR data (cm^{-1}) for **5**: Re═O: 986 (s), 966 (s); Re−S: 1463 (s), 1440 (m); arom: 754 (s), 730 (s), 720 (s). [c] Obtained in insufficient amount.

Table 2. Crystal Data and Structure Refinements for **2**, **3**, and **5**−**8**

compound	{MeReO(edt)}$_2$, **2**	{MeReO(pdt)}$_2$, **3**	{MeReO(mtp)}$_2$(μ-OH), **7**	{ReO}$_2$(edt)$_3$, **6**	{ReO}2(mtp)$_3$, **5**	{$MeReO_2$}$_2$(dte), **8**
empirical formula	$C_6H_{14}O_2Re_2S_4$	$C_8H_{18}O_2Re_2S_4$	$C_{32}H_{55}NO_3Re_2S_4$	$C_6H_{12}O_2Re_2S_6$	$C_{24}H_{21}O_2Re_2S_6$	$C_6H_{12}O_6Re_2S_2$
formula weight	618.81	646.86	1002.41	680.92	906.17	616.68
space group	*P*2(1)/*c*	*P*2$_1$/*n*	*P*2/*c*	*P*2(1)/*c*	*C*2/*c*	*P*-1
unit cell dimensions, Å and deg	a = 9.479(2) b = 11.612(3) c = 12.625(3) β = 110.341(4)	a = 10.4532(5) b = 12.8649(7) c = 10.9873(6) β = 91.093(1)	a = 10.8441(8) b = 9.2669(6) c = 20.9735(13) β = 117.528(10)	a = 8.9073(17) b = 15.065(3) c = 11.347(2) β = 107.996(4)	a = 35.2466(18) b = 7.5740(4) c = 20.8584(11) β = 106.993(1)	a = 6.0438(6) b = 7.3445(8) c = 7.8400(8) α = 76.275(2) β = 87.151(2) γ = 69.755(2)
volume, Å^3	1303.0(5)	1477.30(13)	1869.0(2)	1448.2(5)	5325.2(5)	316.98(6)
density (calcd), mg/m^3	3.154	2.908	1.781	3.123	2.261	3.230
Z	4	4	2	4	8	1
Mo Kα, λ, Å	0.710 73	0.710 73	0.710 73	0.710 73	0.710 73	0.710 73
μ, mm^{-1}	19.177	16.922	6.725	17.548	9.577	19.413
final R indices [$I > 2\sigma(I)$][a]	R1 = 0.0442, wR2 = 0.1102	R1 = 0.0229, wR2 = 0.0658	R1 = 0.0293, wR2 = 0.0855	R1 = 0.0251, wR2 = 0.0509	R1 = 0.0250, wR2 = 0.0533	R1 = 0.0608, wR2 = 0.1575
R indices (all data)[a]	R1 = 0.0590, wR2 = 0.1174	R1 = 0.0235, wR2 = 0.0661	R1 = 0.0354, wR2 = 0.0887	R1 = 0.0369, wR2 = 0.0534	R1 = 0.0343, wR2 = 0.0554	R1 = 0.0619, wR2 = 0.1590

[a] $R1 = \sum||F_o| - |F_c||/\sum|F_o|$; $wR2 = \{\sum[w(F_o^2 - F_c^2)^2]/\sum[w(F_o^2)^2]\}^{1/2}$.

diffraction grew at the interface over 2 days. The diffraction study showed that an ionic compound had formed, but the amount obtained was insufficient (estimated <10%) for elemental analysis. Such a minor compound would perhaps not be worth considering further, save that its structure turns out to be unprecedented.

{$MeReO_2$}$_2$(dte), 8. *Method 1*. Dithioerythritol (0.118 g, 0.77 mmol) was dissolved in 5 mL of methylene chloride and 10 mL of toluene which was heated and added all at once to the $MeReO_3$ solution. The reaction was allowed to stir for 20 min in an ice bath, and then was stirred under ambient conditions for 5 h. The reaction mixture was transferred to a new flask, layered with hexane, and held at −22 °C for 5 days. Dark red crystals were collected by suction filtration, washed with 10 mL of hexanes, and dried. *Method 2*: $MeReO_3$ (50 mg, 0.2 mmol) was added into 10 mL of toluene containing dithioerythritol (15.4 mg, 0.1 mmol). The mixture was stirred for 2 h as the color changed to deep red. The solution was concentrated to 1 mL under vacuum. Then 5 mL of hexanes was layered on this mixture which was left in the freezer for 1 day. Red crystals were obtained in 78% yield by filtration and washed with hexanes.

Characterization. The elemental analyses and NMR spectra, ^{1}H and ^{13}C, of the new compounds are given in Table 1. The analytical data match the molecular formulas within accepted tolerances. The NMR spectra present no remarkable features. In some compounds, e.g., **5**, many distinct resonances present themselves because the protons in the structure are diastereotopic.

Crystallography. The parameters obtained from single-crystal X-ray studies are summarized in Table 2. Crystal data and details of X-ray structure determination for **2**, **3**, and **5**−**8** are given there. Intensity data collections for all structures were performed on a Bruker SMART 1000 diffractometer (CCD detector, Mo Kα radiation, graphite monochromator, hemisphere algorithm (for **3** and **5**: 1286 frames)/full-sphere algorithm (for **2**, **6**−**8**: 1818 frames) with 50 additional frames for decay correction, crystal-detector distance 5.02 cm, 0.3° scans in ω with an exposure time from 10 to 30 s per frame for different experiments). The positions of heavy atoms were found by the direct methods. The remaining non-hydrogen atoms were located in an alternating series of least-squares cycles and difference Fourier maps. All non-hydrogen atoms were refined in full-matrix anisotropic approximation. All hydrogen

atoms were placed in the structure factor calculation at idealized positions and were allowed to ride on the neighboring atoms with relative isotropic displacement coefficients.

Equilibrium and Kinetics. These parameters were evaluated spectrophotometrically in benzene at 25 °C. The reactions between **1**−**3** and triphenylphosphine produce the mononuclear compounds MeReO(dithiolate)PPh_3. Repetitive scans show the buildup of absorbance in the range 330−500 nm. The absorption maximum of the product from **3** is 407.5 nm ($\epsilon = 5.73 \times 10^3$ L mol^{-1} cm^{-1}); from **2**, 398.5 nm (2.74×10^3); from **1**, 400 (sh, $\sim 1.5 \times 10^3$) and 340 nm (max, 2.7×10^3). With 10−30 mM PPh_3, the reactions went to completion, and no evidence was obtained for any remaining amount of the starting dimer. With 4-phenylpyridine, on the other hand, an equilibrium was attained. The equilibrium constants for these reactions were obtained by analysis of the equilibrium absorbance values as a function of [4-PhPy] according to

$$\mathrm{Abs} = \epsilon_{\mathrm{ML}}\left\{\sqrt{\frac{K_3^2[\mathrm{L}]^4}{16} + K_3[\mathrm{L}]^2[\mathbf{D}]_0} - \frac{K_3[\mathrm{L}]^2}{4}\right\} \qquad (2)$$

where K_3 pertains to the reaction

$$\{\mathrm{MeReO(dithiolate)}\}_2 + 2\mathrm{NC_5H_4Ph} \rightleftharpoons 2\mathrm{MeReO(dithiolate)NC_5H_4Ph} \qquad (3)$$

and the absorbance from **1**−**3** ($\epsilon \sim 120$ L mol^{-1} cm^{-1}) near λ 400 nm has been neglected since ϵ_{ML} is 1.1×10^4 L mol^{-1} cm^{-1} for MeReO(edt)(4-Phpy). The values of ϵ_{ML} and K_3 were obtained by nonlinear least-squares fitting of the absorbance values to eq 2 as a function of [L].

Although triphenylphosphine is a much better Lewis base than 4-phenylpyridine toward **1**−**3**, it reacts much more slowly. In the range 10−30 mM PPh_3, the reactions required ≥30 h to reach completion, whereas 1−8 mM PhC_5H_4N equilibrates with **3** within ca. 1 h, much as was the case with the same ligand and **1**.[3] Quite remarkably, however, **2** reacts with PhC_5H_4N so rapidly that stopped-flow techniques were required. The spectrophotometric measurements were carried out with Shimadzu 2101 and 3101 spectrophotometers and the stopped-flow studies with the OLIS rapid-scanning spectrometer. All kinetic experiments employed the ligand in $\geq 10^2$-fold excess, and thus conformed to first-order kinetics. Values of the pseudo-first-order rate constants were obtained by nonlinear least-squares fitting to

$$\mathrm{Abs}_t = \mathrm{Abs}_\infty + (\mathrm{Abs}_0 - \mathrm{Abs}_\infty)\exp(-k_\psi t) \qquad (4)$$

Results and Interpretation

Structural Data. Figures 1−3 display the respective molecular structures for one compound of each new type: **5**, **7**, and **8**; Figures S-1 and S-2 present structures of **2** and **3** (not shown in the main text because **1** was previously depicted),[1] and Figure S-3 shows **6**. In all of these compounds save **7** the oxorhenium(V) atom lies slightly above the basal plane of an approximate square pyramid. This geometry reflects the strong π back-bonding from the oxo group to rhenium. Ligation in the sixth (axial) position can be forced with a strong donor ligand, but it is less preferable. Only in the case of a chelating ligand such as 2,2′-bipyridine, 1,10-phenanthroline, or 1,2-bis(diphenylphosphino)benzene is approximately octahedral six-coordination attained.[8]

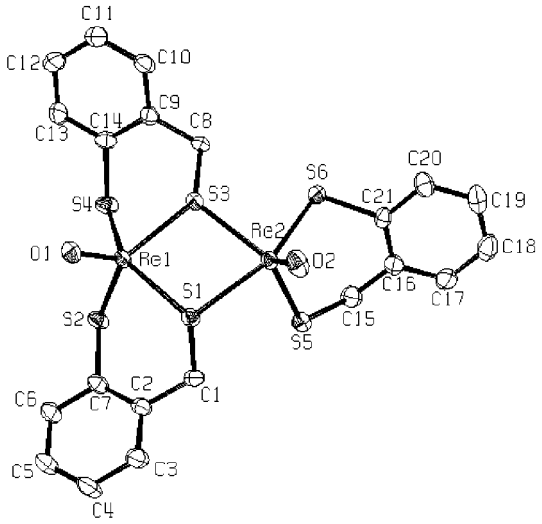

Figure 1. Molecular structure of $\{ReO\}_2(mtp)_3$, **5**. Structural parameters are given in Table 4.

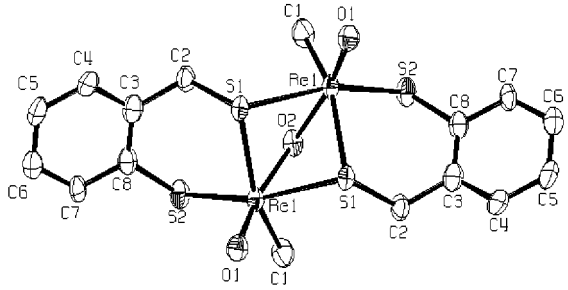

Figure 2. Perspective view of **7** with thermal ellipsoids at the 40% probability level. Structural parameters are given in Table 5.

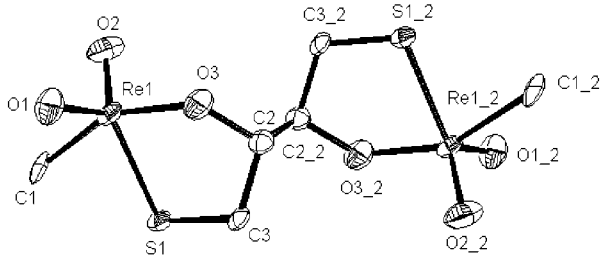

Figure 3. Molecular structure of $\{MeReO_2\}_2(dte)$, **8**. Structural parameters are given in Table 6.

Some important bond lengths and angles are summarized in Table 3 for $\{MeReO(dithiolate)\}_2$, **1**−**3**, in Table 4 for $\{ReO\}_2(dithiolate)_3$, **5**−**6**, in Table 5 for $\{MeReO(mtp)\}_2$-(μ-OH), **7**, and in Table 6 for $\{MeReO_2\}_2(dte)$, **8**. The rhenium(V)−oxygen distances to the oxo group in **1**−**3** and **5**−**7** lie in a narrow range, 167.2−168.0 pm; the mean distance is 167.6 pm and is constant well within the statistical error of 3σ. This short distance signifies a strong interaction; according to the symmetry of the nonbonding orbitals on oxygen in an MO analysis it is properly regarded as a rhenium−oxygen triple bond.[9] (Nonetheless, an Re═O notation sometimes offers an advantage.[10]) Even in the

(8) Espenson, J. H.; Shan, X.; Lahti, D. W.; Rockey, T. M.; Saha, B.; Ellern, A. *Inorg. Chem.* **2001**, *40*, 6717−6724.

Table 3. Selected Bond Lengths (pm) and Angles (deg) for {MeReO(edt)}$_2$, **2**, {MeReO(pdt)}$_2$, **3**, and {MeReO(mtp)}$_2$, **1**

	{MeReO(edt)}$_2$, **2**	{MeReO(pdt)}$_2$, **3**	{MeReO(mtp)}$_2$, **1**[a]
Re(1)−O(1)	167.6(7)	167.2(4)	167.4(3)
Re(1)−C(1)	213.5(8)	213.9(6)	212.7(5)
Re(1)−S(3) (br)	238.1(2)	237.58(14)	239.36(11)
Re(1)−S(2)	235.5(2)	236.40(13)	236.07(11)
Re(1)−S(1)	226.3(2)	227.50(15)	229.05(11)
O(1)−Re(1)−C(1)	105.7(4)	106.3(3)	107.1(2)
O(1)−Re(1)−S(1)	110.5(2)	107.97(16)	107.02(12)
C(1)−Re(1)−S(1)	83.6(3)	79.62(19)	80.23(13)
O(1)−Re(1)−S(2)	113.5(2)	112.81(17)	115.88(13)
C(1)−Re(1)−S(2)	140.7(3)	140.36(19)	136.84(15)
S(1)−Re(1)−S(2)	84.61(8)	94.16(5)	90.81(4)
O(1)−Re(1)−S(2)	113.5(2)	112.81(17)	108.82(12)
C(1)−Re(1)−S(3)	88.3(3)	87.35(18)	87.89(13)
S(2)−Re(1)−S(3)	76.21(18)	73.85(5)	75.05(4)
Re(1)−S(2)−Re(2)	100.08(9)	101.97(5)	101.47(4)
S(1)−Re(1)−S(3)	138.92(9)	141.18(5)	144.13(4)

[a] From ref 1.

Table 4. Selected Bond Lengths (pm) and Angles (deg) for {ReO}$_2$(edt)$_3$, **6**, and {ReO}$_2$(mtp)$_3$, **5**

	{ReO}$_2$(edt)$_3$, **6**	{ReO}$_2$(mtp)$_3$, **5**
Re(1)−O(1)	167.2(4)	167.6(3)
Re(1)−S(2)	228.53(18)	230.97(12)
Re(1)−S(1)	236.50(16)	237.65(12)
Re(1)−S(3)	236.68(15)	237.43(11)
Re(2)−O(2)	167.9(4)	168.3(3)
Re(2)−S(5)	226.37(15)	225.53(13)
Re(2)−S(1)	239.80(15)	241.39(12)
O(1)−Re(1)−S(2)	110.08(17)	107.12(12)
S(4)−Re(1)−S(2)	86.80(7)	81.23(4)
O(1)−Re(1)−S(1)	110.13(16)	109.95(11)
S(4)−Re(1)−S(1)	141.05(6)	141.67(5)
S(2)−Re(1)−S(1)	84.81(6)	91.29(4)
O(2)−Re(2)−S(5)	108.56(15)	112.72(12)
S(5)−Re(2)−S(6)	86.47(6)	91.62(4)
O(2)−Re(2)−S(1)	107.09(14)	104.22(11)
S(5)−Re(2)−S(1)	88.56(5)	85.04(4)
S(6)−Re(2)−S(1)	143.19(6)	149.55(4)
S(1)−Re(1)−S(3)	76.95(5)	74.91(4)
Re(1)−S(1)−Re(2)	100.43(5)	102.16(4)

Table 5. Selected Bond Lengths (pm) and Angles (deg) for {MeReO(mtp)}$_2$(μ-OH), **7**

	{MeReO(mtp)}$_2$(μ-OH), **7**
Re(1)−O(1)	168.0(4)
Re(1)−C(1)	215.3(5)
Re(1)−O(2)	218.5(3)
Re(1)−S(2)	233.69(13)
Re(1)−S(1)	243.30(13)
Re(1)−S(1)#1	245.41(12)
O(1)−Re(1)−O(2)	168.75(12)
O(1)−Re(1)−S(2)	102.35(12)
C(1)−Re(1)−S(1)	154.44(18)
S(2)−Re(1)−S(1)#1	161.17(5)
Re(1)−O(2)−Re(1)#1	99.89(17)

dioxorhenium(VII) compound **8**, the rhenium−oxygen distances (168.1 and 169.3 pm) are also short.

In all of these cases, the compound adopts the syn structure, as shown: In related cases, the syn structures have

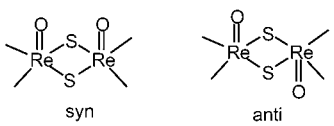

been found to be the more stable thermodynamically.[11−16] In some, the anti form can be obtained, but it is metastable with respect to isomerization, usually acid or base catalyzed.

Table 6. Selected Bond Lengths (pm) and Angles (deg) for {MeReO$_2$}$_2$(dte), **8**

	{MeReO$_2$}$_2$(dte), **8**
Re(1)−O(2)	168.1(11)
Re(1)−O(1)	169.3(10)
Re(1)−O(3)	186.3(11)
Re(1)−C(1)	216.6(13)
Re(1)−S(1)	234.3(3)
O(2)−Re(1)−O(1)	113.4(5)
O(2)−Re(1)−O(3)	104.5(5)
O(1)−Re(1)−O(3)	105.1(5)
O(2)−Re(1)−C(1)	88.0(5)
O(1)−Re(1)−C(1)	93.2(5)
O(3)−Re(1)−C(1)	151.0(4)
O(2)−Re(1)−S(1)	125.3(4)
O(1)−Re(1)−S(1)	118.5(4)
O(3)−Re(1)−S(1)	77.9(3)
C(1)Re−(1)−S(1)	73.6(3)

The six Re(V) compounds, excluding **7**, feature a central, diamondlike unit. We note these features where the additional bridging atom leads to further but easily understood distortions. First, as summarized in Table 7, the two rhenium atoms lie well outside bonding distance to one another. That distance is remarkably constant, between 363.1 and 372.7 pm, indicating the core is relatively invariant in structure. The same is found to be true when one examines the other structural parameters: the two dihedral angles and the Re−S bonds within the core. The Re atoms lie above the mean basal plane defined by S, S, S, and C; the distances are 70.4 (**1**), 77.6 (**2**), and 74.5 (**3**) pm.

In **7** there is a C_2 symmetry axis down the μ-OH group; the presence of that group, an additional bridging ligand, causes a sharpening of the dihedral angles. The one is 61.5° between the two S−Re−S triangles, along the imaginary Re−Re axis; the other is 57.1° between the two Re−S−Re triangles, along the imaginary S−S axis. The Re−Re nonbonded distance in **7** has shortened to 344.4 pm, reflecting the contraction of the diamond by the additional bridging group. The Re−O−Re angle in **7** is 99.9(2)°, and the Re−O distance to the hydroxo group is 218.5(3) pm, clearly indicative of a single bond. Concomitantly, the Re−S−

(9) Nugent, W. A.; Mayer, J. M. *Metal-Ligand Multiple Bonds*; Wiley-Interscience: New York, 1988.
(10) Structural formulas of the oxorhenium(V) compounds are drawn in VB notation, with Re═O double bonds, rather than Re≡O, which represents the MO notation. [Nugent, W. A.; Mayer, J. M. *Metal-Ligand Multiple Bonds*; Wiley-Interscience: New York, 1988.] The lack of formal charges in the VB is advantageous, Re═O vs $^-$Re≡O$^+$, since the latter does not always reflect chemical reactivity; it also allows a readier assignment of oxidation states to various derivatives and products. Our adoption of this notation is not meant to argue that the "real" electronic structure can be better represented by a VB picture.
(11) Cai, S.; Hoffman, D. M.; Wierda, D. A. *Inorg. Chem.* **1991**, *30*, 827−831.
(12) Hahn, M.; Wieghardt, K.; Swiridoff, W.; Weiss, J. *Inorg. Chim. Acta* **1984**, *89*, L31−L32.
(13) Wieghardt, K.; Hahn, M.; Swiridoff, W.; Weiss, J. *Inorg. Chem.* **1984**, *23*, 94−99.
(14) Wieghardt, K.; Hahn, M.; Swiridoff, W.; Weiss, J. *Angew. Chem.* **1983**, *95*, 499−500.
(15) Wieghardt, K.; Guttmann, M.; Chaudhuri, P.; Gebert, W.; Minelli, M.; Young, C. G.; Enemark, J. H. *Inorg. Chem.* **1985**, *24*, 3151−3155.
(16) Schreiber, P.; Wieghardt, K.; Floerke, U.; Haupt, H. J. *Inorg. Chem.* **1988**, *27*, 2111−2115.

Table 7. Nonbonding and Bonding Distances (pm) and Angles (deg) within the Diamondlike Core of the Oxorhenium(V) Compounds

compd	nonbonding Re···Re dist	dihedral angle[a]	dihedral angle[b]	core Re−S dist	Re above mean basal plane (pm)	S,S,O cone angle
1	370.7	160.8	155.6	236.7, 239.4	70.4	65.65
2	363.1	154.0	148.0	235.5, 238.1	77.6	63.17
3	368.0	152.6	144.9	236.4, 237.6	74.5	65.80
5	372.7	159.4	153.6	237.4, 237.6		
6	366.0	153.9	153.9	236.5, 236.7		
7	334.4	122.9	118.5	243.3, 245.4		

[a] Between the two Re−S−Re triangles, along the imaginary S−S axis. [b] Between the two S−Re−S triangles, along the imaginary Re−Re axis.

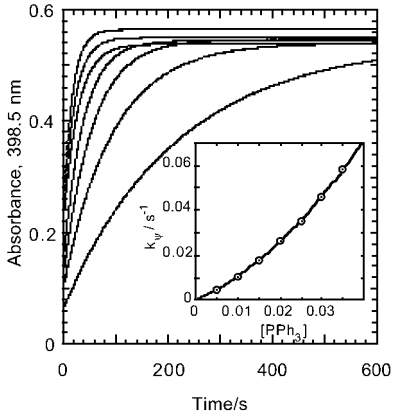

Figure 4. Product formation curves at 398.5 nm for the reaction between 0.1 mM **2** and 3−35 mM PPh_3. The inset shows the fit of the k_ψ values to eq 5.

Re angle decreases to 86.4(4)° (cf. 101° in **1**) and the S−S nonbonded distance grew to 306 pm, compared to 290 pm in **1**.

Equilibrium and Kinetics of the Monomerization Reactions. Compounds **1**−**3** are subject to conversion to mononuclear species by reactions with exogenous ligands, according to eq 2. These reactions have been extensively studied for pyridines, phosphines, and selected other ligands.[3] With the new dimeric rhenium compounds we have carried out a limited number of studies with two representative ligands, 4-phenylpyridine and triphenylphosphine. As with **1**, the pyridine reactions attained an equilibrium. The values of the equilibrium constants determined from data analysis according to eq 2 are these: $K_3/10^3$ L mol^{-1} are 1.15(3) (**1**),[3] 1.24(4) (**2**), and 1.03(16) (**3**). Within the precision of the measurements, the equilibrium constants for monomer formation with L = 4-phenylpyridine are the same for **1**−**3**. Figure S-4 presents the analysis of the equilibrium data in graphical form.

The kinetics is distinctively different: 4-PhC_5H_4N reacts with **2** *much* more rapidly than with **1** or **3**. In all three cases, however, the form of the rate law is the same, with terms corresponding to first-order and second-order pyridine dependences:

$$k_\psi = k_a[L] + k_b[L]^2 \qquad (5)$$

Because the pyridine reactions are not quite complete at the concentrations used, a constant allowing for the reverse reaction can be appended to eq 5. Figure 4 shows the product formation curves for the reaction between **2** and 4-PhPy and the fit of the k_ψ values to eq 3. Other graphs representing the kinetic data are presented in Figures S-5 to S-11. Values of the rate constants for both ligands are summarized in Table 8. Two points should be emphasized, as mentioned previously: k_b is abnormally large for **2** as compared to the others, and the phosphine reacts more slowly than the pyridine.

Table 8. Summary of Rate Constants[a] for the Monomerization of the Dimers **1**−**3** with 4-Phenylpyridine and Triphenylphosphine

	4-PhC_5H_4N		PPh_3	
	k_a/L mol^{-1} s^{-1}	k_b/L^2 mol^{-2} s^{-1}	k_a/L mol^{-1} s^{-1}	k_b/L^2 mol^{-2} s^{-1}
1[b]	≤1	7.0(6)	0.0157(5)	0.051(6)
2	22(20)	2.04(8) × 10^4	0.83(1)	23.7(4)
3	0.17(3)	35(4)	0.013(1)	0.18(4)

[a] The uncertainties represent the standard error from the fit to the two-term expression, eq 5; when the error is large (e.g., k_a for **2**), the implication is that this term is barely if at all significant. [b] From ref 3.

Catalysis of Oxygen Reduction. Compound **6**, as reported earlier for **5**,[6] catalyzes the oxidation of alkyl and aryl phosphines by O_2. These reactions were easily detected by ^1H and ^{31}P NMR spectroscopy. What makes this conversion remarkable is that compounds **1**−**3**, with similar structures (a) do not react with oxygen, (b) do not activate oxygen, but (c) do participate in oxygen atom transfer reactions, e.g., eq 6,[17] that function equally well in the presence as in the absence of O_2.

$$PicO + PPh_3 \rightarrow Pic + Ph_3PO \qquad (6)$$

The data reported here refer specifically to 4-methylpyridine *N*-oxide. Reactions analogous to eq 6, which were not studied quantitatively, occur for a wide range of other pyridine *N*-oxide derivatives. Given the previous study of **6**, only a few experiments on oxygen activation by **5** were carried out. It should be noted, of course, that the much more sluggish activation of O_2 for phosphine oxidation can be attained with $MeReO_3$ (MTO) as a catalyst.[18] In that instance a different mechanism operates, however, and the phosphine must first abstract an oxygen atom from the oxorhenium(VII) compound, which poses a substantial kinetic barrier.

Compound 7. Compounds containing the unit $Re_2(\mu\text{-OH})$ were not previously known. The closest analogue may be the tetranuclear amidato compound $[Re_4(PhNCOMe)_6Cl(\mu\text{-O})(\mu\text{-OH})(MeOH)_3](ReO_4)_2$, **9**, with Re^{III}−OH distances of 206(3) and 229(2) pm,[19] comparable to 218.5 pm for **7**. Compound **9** has Re−(μ-O) distances of 188 and 194 pm. Other pertinent μ-oxo compounds and their Re−(μ-O) distances are these: $[Re_2O_4(CH_2CMe_3)_4(\mu\text{-O})]$ (d = 190, 194 pm),[5] $[Re_2O_2(CH_2CMe_3)_4(\mu\text{-O})]$ (d = 186−198 pm),[20]

(17) Wang, Y.; Espenson, J. H. *Org. Lett.* **2000**, *2*, 3525−3526.
(18) Eager, M. D.; Espenson, J. H. *Inorg. Chem.* **1999**, *38*, 2533−2535.
(19) Cotton, F. A.; Lu, J.; Huang, Y. *Inorg. Chem.* **1996**, *35*, 1839−1841.

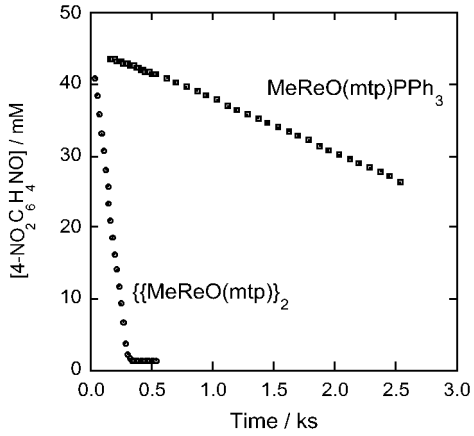

Figure 5. Progress of the catalyzed reaction between 44.2 mM 2-methyl-4-nitropyridine *N*-oxide and 44.2 mM PPh_3, eq 6, with 1.0 mM MeReO(mtp)PPh_3(top) and 0.25 mM **1**.

$[Re_2(\mu\text{-}CH_2)O_2Me_4(PMe_3)_2(\mu\text{-}O)]$ (d = 188, 197 pm),[21] and $[Re_2(\mu\text{-}CH_2)O_2Me_4(\mu\text{-}O)]$ (d = 190, 194 pm).[21] Independent of the reaction used to form **7**, given in eq 1, it is known that **1** can simply be converted with Bu^n_4NCl to the stable chloro monomer MeReO(mtp)Cl^-, comparably stable to MeReO(mtp)PPh_3, by a reaction like eq 2, L = Cl^-. Moreover, **1** does not react with Bu^n_4NOH in benzene, suggesting that chloride plays a role, as yet not disclosed, in the success of eq 1. We note that partially opened dimeric structures have been found[2] and postulated.[3] An attempt was made to prepare a μ-SH analogue of **7**, but no reaction occurred between **1** and H_2S in benzene.

Catalyzed Oxygen Atom Transfer. Reaction 6 does not occur over long times in the absence of a catalyst, but is catalyzed by MeReO(mtp)PPh_3 and by **1**. The latter is much more effective; Figure 5 shows that 0.25 mM **1** is 90 times a better catalyst than 1.0 mM MeReO(mtp)PPh_3 under the conditions specified.

Kinetics studies showed that the reaction is first order with respect to [**1**]. Compound **1** is so effective as a catalyst in this reaction that its concentration was typically held at 16.7 μM in the next series of experiments. The reaction is also first order with respect to [PicO] at relatively high (and thus constant) values of [PPh_3]. At lower [PPh_3], where its concentration is not constant, the time variation of the fraction [PicO]/[PPh_3] needs to be considered. The numerator provides the first-order dependence on [PicO]. The denominator is also decreasing with time, as PPh_3 is consumed. Thus the *apparent* order with respect to [PicO] can appear to be >1, but that is an artifact of the form used. In any event, initial rate kinetics was used for the further analysis. The initial rate over the full range of phosphine concentrations decreases with [PPh_3] according to the following rate law which contains the suggested inverse phosphine dependence:

$$v = \frac{k[\mathbf{1}][\mathrm{PicO}]}{1 + \kappa[\mathrm{PPh_3}]} \qquad (7)$$

The fit of the initial rates to this functional form is illustrated in Figure 6 and yields these parameters: $k = 5.8 \times 10^6$ L mol^{-1} s^{-1} and $\kappa = 3.5 \times 10^2$ L mol^{-1} at 25 °C in benzene.

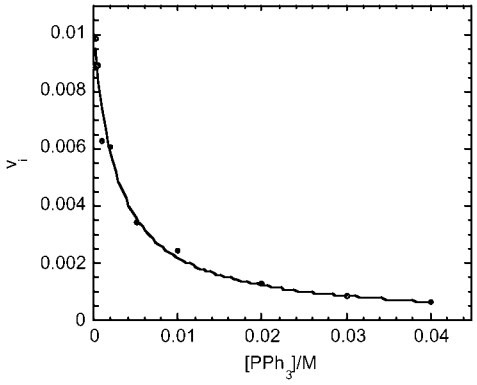

Figure 6. Illustrating rate retardation by increasing concentrations of triphenylphosphine in a series of reactions starting with 0.1 mM picoline *N*-oxide and 16.7 μM **1** at the catalyst. Data were taken at 25 °C in benzene. The data fit displayed is for eq 7.

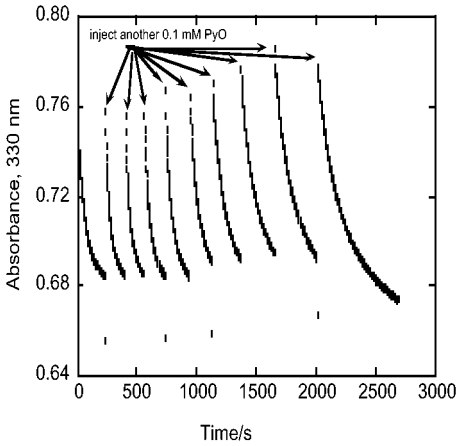

Figure 7. Series of experiments depicting the decrease of the absorbance of PicO as successive portions of it are injected into a solution with $[PPh_3]_0$ = 20.0 mM and $[\mathbf{1}]_0$ = 16.7 μM. The decrease in the rate constant with time matches the decrease in [**1**] from monomerization.

The value of κ is sufficiently large that the rate rises sharply at low [PPh_3]; the decrease in its concentration during an experiment at low phosphine could give rise to an apparent (but literally incorrect) reaction order >1 with respect to the concentration of [PicO].

A different series of experiments was done by injecting successive portions of one limiting reagent or the other, PicO or PPh_3, into a solution containing catalyst **1** and the other reagent. Figure 7 shows the successive injection of 0.1 mM portions into solutions that contain a large (20 mM) excess of phosphine, and Figure S-12 presents the series with injections of phosphine. In both, the decrease of the absorbance of PicO follows first-order kinetics in each reaction segment. The rate constant rises between the first curve and the second, and then steadily declines (insert, Figure 7). This unusual phenomenon parallels the increase in the concentration of the less reactive monomer MeReO(mtp)PPh_3, which grows as time progresses. From the rate constants k_a and k_b (eq 5 and Table 8) one can calculate [**1**] and [MeReO(mtp)PPh_3] during the reaction time. That is, a different value of k was expected, according to [**1**], at the time each injection of PicO was made. We carried out an analysis comparing the change in k to these two variables. The two profiles match satisfactorily, as presented in Figure 8, substantiating this

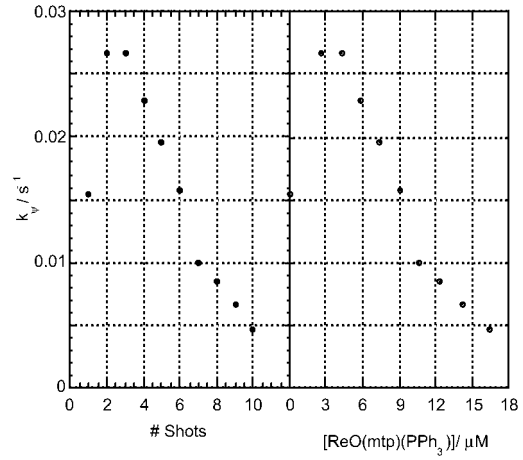

Figure 8. Comparison of rate constants for each curve in Figure 7 against concentration of MeReO(mtp)PPh_3, as calculated from rate constants in Table 8 and elapsed time intervals between injections of PicO.

interpretation. During any one of these catalytic cycles, [**1**] remains constant because the reaction time is so short. When a series is done in tandem, however, the longer time interval allows the partial conversion of **1** to MeReO(mtp)PPh_3.

Discussion

Monomerization Reactions. Given the extensive data for reactions between **1** and L = NC_5H_4R [3] and PAr_3,[3,22] several aspects of the new data for the parallel reactions of **2** and **3** came as no surprise. As with **1**, $k_a^{Py} \gg k_a^{P}$ and $k_b^{Py} \gg k_b^{P}$. This counters the thermodynamic trend, given $K_8 = 3 \times 10^{-3}$ for eq 8 (determined for **1**, but valid also for **2**−**3**, because the three have the same value of K_3):

$$\text{MeReO(dithiolate)PPh}_3 + \text{NC}_5\text{H}_4\text{-4-Ph} \rightleftharpoons \text{MeReO(dithiolate)NC}_5\text{H}_4\text{-4-Ph} + \text{PPh}_3 \quad (8)$$

In our original study we suggested a chemical mechanism (see eqs 3−6 of ref 3) that we now wish to modify in one respect, to avoid postulating four-coordinate MeReO(dithiolate) as an intermediate. At the same time, the revised scheme may advance the understanding of these relative rates, **2** ≫ **1**, **3**, an inequality that holds for both k_a and k_b. Scheme 1 shows the proposed chemical mechanism for monomerization. According to the parameter designations, $k_a = k_3K_1$ and $k_b = k_4K_1K_2$. In an approximate sense, one might factor k_a and k_b into two effects: (a) facile and reversible bonding of L to the lower axial position of the dimer, represented by K_1 and K_2, and (b) the rate constants k_3 and k_4 for the unimolecular scission of the Re→S coordinate bonds. If, for L = 4-PhPy, one takes $K_1/K_2 = 24$ (the ratio for L = PyO),[3] then k_3/k_4 is 0.2 (for **2**) or 0.8 (for **3**). It appears therefore that nearly all the reactivity difference resides in the equilibrium constants. This comes to be of particular importance with regard to **1** as a catalyst for OAT. The k_b pathway is the only important one for **1**; these data show that significant concentrations of MeReO(mtp)$(OPic)_2$ will not form at the low [PicO] used for the study of OAT kinetics.

Scheme 1. Proposed Mechanism for Monomerization

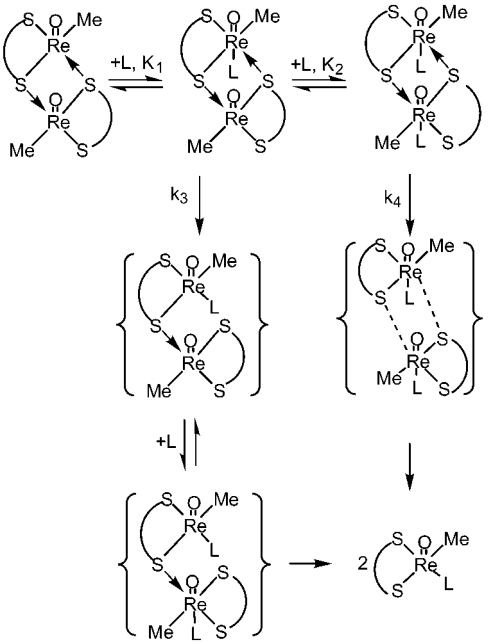

OAT Catalysis by Dimers 1. OAT reactions, eq 6, show significant rate enhancements when **1** is the catalyst as compared to MeReO(mtp)PPh_3, as displayed in Figure 5.[17] A key step with the mononuclear catalyst is ligand replacement:

$$\text{MeReO(mtp)PPh}_3 + \text{PicO} \leftrightarrows \text{MeReO(mtp)OPic} + \text{PPh}_3 \; (K_9 = k_9/k_{-9}) \quad (9)$$

This reaction is unfavorable (estimated $pK_9 \sim 2-3$) and slow (estimated $k_9 \sim 10^{-3}$ L mol^{-1} s^{-1}). Later in the catalytic cycle, a steady-state dioxorhenium(VII) intermediate forms and is then returned to the parent phosphine (but not to the product of eq 9, owing to kinetic selectivity in favor of phosphine). Thus in nearly every pass through the cycle this barrier is reencountered, which provides one reason the monomeric rhenium(V) complex is a less efficient catalyst.

With the dimer catalyst, on the other hand, monomerization by phosphine is slow relative to OAT catalyzed by **1**. Thus the dimer remains intact and can act as a catalyst by an independent route. A sound inference is that none of intermediate forms of **1** give monomers either, as they would revert irreversibly to MeReO(mtp)PPh_3. The suggested set of preequilibrium and kinetic steps are these: (a) the rapid, stepwise addition of PicO to an axial position on Re(V) with previously known equilibrium constants $K_{a1} = 4.1 \times 10^3$ and $K_{a2} = 1.7 \times 10^2$ L mol^{-1};[3] (b) rapid equilibration between **D**−OPic and PPh_3, with $K_b = \kappa = 3.5 \times 10^2$ L mol^{-1} (evidently, the coordination of one PicO "opens" the structure of **D** so as to accommodate PPh_3 because formation of **D**−PPh_3 is negligible on its own); and a competing pair of two unimolecular rate-controlling steps, (c) and (d), no doubt each

(20) Cai, S.; Hoffman, D. M.; Huffman, J. C.; Wierda, D. A.; Woo, H.-G. *Inorg. Chem.* **1987**, *26*, 3693−3700.
(21) Hoffman, D. M.; Wierda, D. A. *J. Am. Chem. Soc.* **1990**, *112*, 7056−7057.
(22) Lahti, D. W.; Espenson, J. H. *J. Am. Chem. Soc.* **2001**, *123*, 6014−6024.

featuring internal nucleophilic assistance, that serve to break the covalent O−N bond and release Pic. These chemical equations represent the proposed sequence of events:

(a) $\mathbf{D} + \mathrm{PicO} \rightleftharpoons \mathbf{D}{-}\mathrm{OPic}\ (K_{a1})$

(b) $\mathbf{D}{-}\mathrm{OPic} + \mathrm{PPh_3} \rightleftharpoons \mathbf{D}(\mathrm{OPic})(\mathrm{PPh_3})\ (\mathbf{A})\ (K_b = \kappa)$

(c) $\mathbf{A} \rightarrow \mathrm{ORe^{V}{\sim}{\sim}Re^{VII}(O)_2(PPh_3)}\ (\mathbf{B}) + \mathrm{Pic}\ (k_c)$

(d) $\mathbf{D}{-}\mathrm{OPic} \rightarrow \mathrm{ORe^{V}{\sim}{\sim}Re^{VII}(O)_2}\ (\mathbf{C}) + \mathrm{Pic}\ (k_d)$

These reactions are then followed by faster ones, specified in greater detail later, in which the dioxorhenium(VII) intermediates **B** and **C** are restored to **D**. The steady-state rate law for the sequence (a)−(d), allowing that both k_c and k_d may provide suitable pathways, is

$$v = \left\{\frac{k_c K_{a1} K_b[\mathrm{PicO}][\mathrm{PPh_3}] + k_d K_{a1}[\mathrm{PicO}]}{1 + K_b[\mathrm{PPh_3}]}\right\}[\mathbf{D}]_T \quad (10)$$

This equation assumes that $K_{a1}[\mathrm{PicO}] \ll 1$ at [PicO] = 0.1−0.5 mM. Given that $K_{a1} = 4.1 \times 10^3$ L mol^{-1}, this approximation holds under the conditions of the kinetics experiments. Because the rate shows no positive order with respect to [PPh_3], the k_c term of eq 10 can be disregarded; evidently **A** is a reversible dead end. Only the second term in the rate law matters; thus k (of eq 7) $= k_d K_{a1} = 5.8 \times 10^6$ L mol^{-1} s^{-1} and $k_d = 1.4 \times 10^3$ s^{-1}. The difference between this sequence of reactions and that without PPh_3 is that **C** is rapidly intercepted by phosphine, but decomposes to MTO and RS−SR without it.

The chemistry of the steps following the rate-controlling step feature a rapid reaction with phosphine, the net result of which is the reduction of dioxorhenium(VII) and subsequent elimination of phosphine oxide. Scheme 2 presents these reaction steps and others needed to complete the catalytic cycle. The details are conjectural, but the model in which coordinated triphenylphosphine oxide intervenes is to be preferred over simple oxygen atom abstraction by phosphine because such an intermediate has been observed directly with molybdenum compounds.[23]

Scheme 2. Proposed Mechanism for Catalysis by Oxorhenium(V) Dimers

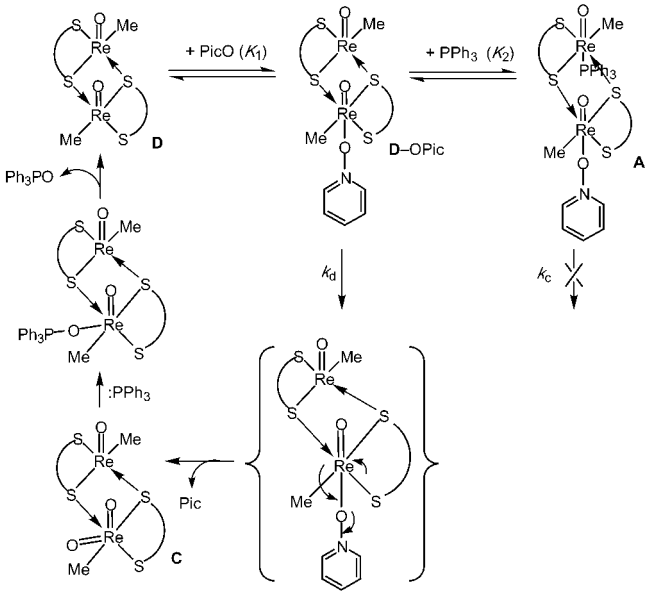

Acknowledgment. This research was supported by a grant from the National Science Foundation. Some experiments were conducted with the use of the facilities of the Ames Laboratory.

Supporting Information Available: Further results from X-ray crystallography and plots of kinetic data to illustrate agreement with selected mathematical forms and to evaluate numerical parameters. This material is available free of charge via the Internet at http://pubs.acs.org.

IC011287J

(23) Smith, P. D.; Millar, A. J.; Young, C. G.; Ghosh, A.; Basu, P. *J. Am. Chem. Soc.* **2000**, *122*, 9298−9299.